Mathematical Modelling and Analysis 2005. Pages 57–64
Proceedings of the 10th International Conference MMA2005&CMAM2, Trakai
 ISBN 9986-05-924-0

AN ALTERNATING-DIRECTION FINITE DIFFERENCE METHOD FOR THREE-DIMENSIONAL FLOW IN UNSATURATED POROUS MEDIA

A. ARRARÁS and J.C. JORGE

Departamento de Matemática e Informática, Universidad Pública de Navarra
Campus de Arrosadía s/n, 31006, Pamplona (Navarra), Spain
E-mail: andres.arraras@unavarra.es; jcjorge@unavarra.es

Abstract. We develop an efficient numerical algorithm for simulating three-dimensional isothermal Darcian flows through isotropic and homogeneous porous media. Such method is obtained by means of two consecutive procedures. Firstly, a modified fractionary implicit Euler method is used to discretize the time variable, decomposing the original problem in three families of nonlinear one-dimensional elliptic problems. Then, this three-level scheme is combined with a finite difference spatial discretization in order to deduce the numerical algorithm. The nonlinear systems of algebraic equations are solved with a quasi-Newton iteration technique, leading to simple sets of tridiagonal linear systems for computing the final solution.

Key words: alternating-direction, porous media, Richards' equation

1. Introduction

Prediction of fluid movement through unsaturated porous media is an important question which concerns to many hydrological processes, including infiltration, soil moisture storage, evaporation, plant water uptake, groundwater recharge, runoff and erosion (see [4, 5, 8]). The interest in water flow phenomena has strongly increased in recent years due to the important role it play in the transport of hazardous wastes towards phreatic layers, which adversely affect the quality of subsurface environment (see [6]).

If we consider an isotropic and homogeneous porous medium, Darcian fluid motion is assumed to obey the classical Richards equation (see [1, 3]). Let Ω be a three-dimensional flow domain with boundary $\partial\Omega = \Gamma$ and set $J = [0, T]$ as the time interval. Consider Richards' equation in the form:

$$\frac{\partial\theta(\psi)}{\partial t} = \nabla\cdot\left[K(\psi)\nabla\psi(\mathbf{x},t)\right] + \frac{\partial K(\psi)}{\partial z} - S(\psi), \quad (\mathbf{x},t)\in\Omega\times J, \tag{1.1}$$

with initial condition

$$\psi(\mathbf{x},0) = \psi_0(\mathbf{x}), \quad \mathbf{x}\in\Omega, \tag{1.2}$$

and boundary conditions

$$\psi(\mathbf{x},t) = \psi_D(\mathbf{x},t), \ (\mathbf{x},t)\in\Gamma_D\times J, \tag{1.3}$$

$$-\left[K(\psi)\left(\nabla\psi(\mathbf{x},t)+\nabla z\right)\right]\mathbf{n}_{\Gamma_N} = \sigma(\mathbf{x},t), \ (\mathbf{x},t)\in\Gamma_N\times J, \tag{1.4}$$

where $\psi(\mathbf{x},t)\,[L]$ is the pressure head, $\theta(\psi)\left[L^3L^{-3}\right]$ is the volumetric moisture content, $K(\psi)\left[LT^{-1}\right]$ $(K(\psi)\geq K_0>0)$ denotes the unsaturated hydraulic conductivity, $S(\psi)\left[T^{-1}\right]$ is a source/sink term (for example, the root water uptake function in soil profiles), $t\,[T]$ is time and $\mathbf{x}\equiv(x,y,z)\,[L]$ refers to the spatial dimensions. Γ_D and Γ_N indicate Dirichlet and Neumann type boundary surfaces ($\Gamma_D\cup\Gamma_N=\Gamma$) and $\mathbf{n}_{\Gamma_N}$ is the outward unit normal vector with respect to Γ_N. The constitutive relationships $\theta(\psi)$, $K(\psi)$ and $S(\psi)$ are defined by a set of nonlinear functions obtained heuristically, determining the highly nonlinear nature of (1.1) (see [1, 4, 7] for a detailed description of these expressions).

In this paper we develop an efficient numerical method for solving (1.1). Firstly, Section 2 describes a modified fractionary implicit Euler scheme for the time semidiscretization, which is combined in Section 3 with a finite difference spatial approximation to deduce the method. In Section 4, a quasi-Newton iteration technique is introduced in order to solve the nonlinear systems of algebraic equations, describing the final numerical algorithm. Finally, Section 5 shows the numerical simulation of a lixiviation process in a variably saturated porous medium.

2. Time Semi-Discretization

Suppose that the solution of equation (1.1) is approximated at time levels $0=t_1<\ldots<t_S=T$ and let $\Delta t^j = t^{j+1}-t^j$ be the corresponding time steps $(j=1,\ldots,S-1)$.

Firstly, we rewrite Richards' equation as follows:

$$\frac{\partial\theta(\psi)}{\partial t} = \mathcal{A}_1(\psi)+\mathcal{A}_2(\psi)+\mathcal{A}_3(\psi)-S(\psi), \tag{2.1}$$

where, omitting some functional dependencies for convenience,

$$\mathcal{A}_1(\psi) = \frac{\partial}{\partial z}\left(K\frac{\partial\psi}{\partial z}\right)+\frac{\partial K}{\partial z} \tag{2.2}$$

is the part of the differential operator which describes the vertical infiltration process (effects of pressure head in the z direction and transport due to gravitation) and

$$\mathcal{A}_2(\psi) = \frac{\partial}{\partial y}\left(K\frac{\partial \psi}{\partial y}\right), \quad \mathcal{A}_3(\psi) = \frac{\partial}{\partial x}\left(K\frac{\partial \psi}{\partial x}\right) \tag{2.3}$$

can be viewed as the terms which define the respective infiltration processes that take part in both dimensions of the horizontal plane (effect of pressure head in the y and x directions).

Starting from an initial condition $\psi_0(\mathbf{x})$ given by (1.2), we firstly consider a modified fractionary implicit Euler method for discretizing the time variable, in order to obtain approximations $\psi^{j+1}(\mathbf{x})$ to the state variable $\psi(\mathbf{x})$ at the $(j+1)$-*th* time level. This technique decomposes the original parabolic problem in three families of nonlinear one-dimensional elliptic problems, generalizing the time semi-discretization used in [6] for two-dimensional problems of this kind. Setting the flow domain $\Omega = [0,a]\times[0,b]\times[0,c]$, we apply the following three-staged procedure:

1. Given $\psi^j(\mathbf{x})$, let $\tilde{\psi}^{j+1}(\mathbf{x})$ be the solution of the two-parameter differential equation (parameters are x, y)

$$\tilde{\theta}^{j+1} - \theta^j = \Delta t^j \left\{\mathcal{A}_1\left[\tilde{\psi}^{j+1}(\bar{x},\bar{y},z)\right] - S\left(\psi^j\right)\right\}, \tag{2.4}$$

$\forall\,(\bar{x},\bar{y}) \in [0,a]\times[0,b]\,, z \in (0,c)$, which also satisfies corresponding boundary conditions (1.3) or (1.4) at $(\bar{x},\bar{y},0)$ and $(\bar{x},\bar{y},c)$, evaluated at $t = t^{j+1}$.

2. Next, from the fictitious state $\tilde{\psi}^{j+1}(\mathbf{x})$ obtained at the previous stage, we define $\hat{\psi}^{j+1}(\mathbf{x})$ as the solution of

$$\hat{\theta}^{j+1} - \tilde{\theta}^{j+1} = \Delta t^j \mathcal{A}_2\left[\hat{\psi}^{j+1}(\bar{x},y,\bar{z})\right], \tag{2.5}$$

$\forall\,(\bar{x},\bar{z}) \in [0,a]\times[0,c]\,, y \in (0,b)$. The solution satisfies corresponding boundary conditions at $(\bar{x},0,\bar{z})$ and $(\bar{x},b,\bar{z})$ for $t = t^{j+1}$.

3. Finally, from the values of $\hat{\psi}^{j+1}(\mathbf{x})$, we obtain the approximations $\psi^{j+1}(\mathbf{x})$ as solutions of

$$\theta^{j+1} - \hat{\theta}^{j+1} = \Delta t^j \mathcal{A}_3\left[\psi^{j+1}(x,\bar{y},\bar{z})\right], \tag{2.6}$$

$\forall\,(\bar{y},\bar{z}) \in [0,b]\times[0,c]\,, x \in (0,a)$, considering again suitable boundary conditions at $(0,\bar{y},\bar{z})$ and $(a,\bar{y},\bar{z})$ with $t = t^{j+1}$.

Notice also that the source/sink term $S(\psi)$ in equation (2.4) is evaluated at the previous time level, in order to improve the convergence rate of the iteration procedure which is given in Section 4 (see [1]). Therefore, this time discretization method can be viewed as a modification of the classical fractionary implicit Euler rule. As $S(\psi)$ is a Lipschitz function, this modified fractional step scheme is also consistent with first order of accuracy and it preserves a stability property under not severe restrictions on the time step Δt. Such restrictions just depend on the Lipschitz constant of $S(\psi)$, similarly to the linearly implicit schemes proposed in [2] for semilinear parabolic problems.

3. Spatial Discretization

In order to develop a fully discretized model, we apply a finite difference technique for approximating the spatial derivatives. Let $\Omega_{h_x h_y h_z}$ be a mesh of the flow domain, defined in the following way:

$$\Omega_{h_x h_y h_z} = \{(x_l, y_m, z_n): \quad l = 1, \ldots, N_x, \;\; m = 1, \ldots, N_y, \;\; n = 1, \ldots, N_z\},$$
$$0 = x_1 < \ldots < x_{N_x} = a, \quad h_x = \max_{1 \leq l \leq N_x - 1} (x_{l+1} - x_l),$$
$$0 = y_1 < \ldots < y_{N_y} = b, \quad h_y = \max_{1 \leq m \leq N_y - 1} (y_{m+1} - y_m),$$
$$0 = z_1 < \ldots < z_{N_z} = c, \quad h_z = \max_{1 \leq n \leq N_z - 1} (z_{n+1} - z_n).$$

The discrete solution ψ_h is defined in the discrete domain $\Omega_{h_x h_y h_z}$ and it is denoted by $\psi_{l,m,n} = \psi_h(x_l, y_m, z_n) \simeq \psi(x_l, y_m, z_n)$. We replace the spatial derivatives by the following approximations:

$$\frac{\partial K}{\partial z}(x_l, y_m, z_n) \simeq \frac{K_{l,m,n+1} - K_{l,m,n-1}}{z_{n+1} - z_{n-1}}, \tag{3.1}$$

$$\frac{\partial}{\partial z}\left(K \frac{\partial \psi}{\partial z}\right)(x_l, y_m, z_n) \simeq \frac{K_{l,m,n+1} + K_{l,m,n}}{z_{n+1} - z_{n-1}} \frac{\psi_{l,m,n+1} - \psi_{l,m,n}}{z_{n+1} - z_n} - \frac{K_{l,m,n} + K_{l,m,n-1}}{z_{n+1} - z_{n-1}} \frac{\psi_{l,m,n} - \psi_{l,m,n-1}}{z_n - z_{n-1}}, \tag{3.2}$$

and analogously for the second derivatives with respect to y and x, included in (2.3). Applying these expressions to the original equations, the fully discretized method on $\Omega_{h_x h_y h_z}$ results:

$$\frac{\tilde{\theta}_n^{j+1} - \theta_n^j}{\Delta t^j} = \frac{1}{\overline{\Delta z_n}}\left(\tilde{K}_{n+1/2}^{j+1} \frac{\tilde{\psi}_{n+1}^{j+1} - \tilde{\psi}_n^{j+1}}{\Delta z_n} - \tilde{K}_{n-1/2}^{j+1} \frac{\tilde{\psi}_n^{j+1} - \tilde{\psi}_{n-1}^{j+1}}{\Delta z_{n-1}}\right) + \frac{\tilde{K}_{n+1/2}^{j+1} - \tilde{K}_{n-1/2}^{j+1}}{\overline{\Delta z_n}} - S_n^j, \tag{3.3}$$

for $n = 2, \ldots, N_z - 1$, where the position subindices l and m have been omitted for clarity and the following notation introduced

$$\overline{\Delta z_n} = \frac{z_{n+1} - z_{n-1}}{2}, \qquad \Delta z_n = z_{n+1} - z_n, \qquad \tilde{K}_{n+1/2}^{j+1} = \frac{\tilde{K}_{n+1}^{j+1} + \tilde{K}_n^{j+1}}{2}.$$

The set of nonlinear equations (3.3) must be completed by adding some expressions for the extreme values $n = 1, N_z$, which depend on corresponding boundary conditions at $z = 0$ and $z = c$.

Analogously, the discretization of (2.5) and (2.6) leads us to

$$\frac{\hat{\theta}_m^{j+1} - \tilde{\theta}_m^{j+1}}{\Delta t^j} = \frac{1}{\overline{\Delta y_m}} \left(\hat{K}_{m+1/2}^{j+1} \frac{\hat{\psi}_{m+1}^{j+1} - \hat{\psi}_m^{j+1}}{\Delta y_m} - \hat{K}_{m-1/2}^{j+1} \frac{\hat{\psi}_m^{j+1} - \hat{\psi}_{m-1}^{j+1}}{\Delta y_{m-1}} \right), \quad (3.4)$$

$$\frac{\theta_l^{j+1} - \hat{\theta}_l^{j+1}}{\Delta t^j} = \frac{1}{\overline{\Delta x_l}} \left(K_{l+1/2}^{j+1} \frac{\psi_{l+1}^{j+1} - \psi_l^{j+1}}{\Delta x_l} - K_{l-1/2}^{j+1} \frac{\psi_l^{j+1} - \psi_{l-1}^{j+1}}{\Delta x_{l-1}} \right), \quad (3.5)$$

for $m = 2, \ldots, N_y - 1$ and $l = 2, \ldots, N_x - 1$, together with some additional equations for the values $m = 1, N_y$ and $l = 1, N_x$, which come from the discretization of specific boundary conditions at $y = 0$, $y = b$ and $x = 0$, $x = a$, respectively.

4. Iterative Resolution Procedure

Because of the nonlinear nature of (3.3), (3.4) and (3.5), an iterative method must be used to obtain numerical approximations for these stages. The method implemented in the present study makes use of the modified Picard (quasi-Newton) iteration technique proposed in [7], which has been shown to provide excellent results in terms of minimizing the mass balance error. According to the method, it is possible to expand the value of θ at the new time, $j+1$, and iteration level, $k+1$, in a truncated Taylor series with respect to ψ about the expansion point $\psi^{j+1,k}$, leading to the expression:

$$\frac{\theta^{j+1,k+1} - \theta^j}{\Delta t^j} = C^{j+1,k} \frac{\psi^{j+1,k+1} - \psi^{j+1,k}}{\Delta t^j} + \frac{\theta^{j+1,k} - \theta^j}{\Delta t^j}, \quad (4.1)$$

where $C\left[L^{-1}\right]$ represents the soil water capacity, defined by

$$C^{j+1,k} = \left[\frac{d\theta}{d\psi} \right]^{j+1,k}. \quad (4.2)$$

Substituting the right-hand side of (4.1) into equation (3.3), we obtain the following general matrix equation:

$$\mathbf{A}_z^{j+1,k} \tilde{\psi}^{j+1,k+1} = \mathbf{b}_z^{j+1,k}, \quad (4.3)$$

where $\mathbf{A}_z$ is a symmetric tridiagonal matrix, $\tilde{\psi}$ denotes the unknown vector and $\mathbf{b}_z$ represents the independent term vector. For each iteration, the final system of linearized algebraic equations is solved by Gaussian elimination. As exposed previously, we obtain similar linear systems for the y and x directions, including corresponding unknown vectors $\hat{\psi}$ and ψ, respectively.

Finally, using an expanded formulation, we can rewrite the systems (4.3) as a set of uncoupled linear subsystems (one for each value of the indices l and m):

$$
\begin{aligned}
&- \frac{\tilde{K}^{j+1,k}_{n-1/2}}{\Delta z_{n-1}} \tilde{\psi}^{j+1,k+1}_{n-1} + \left(\frac{\overline{\Delta z_n}}{\Delta t^j} \tilde{C}^{j+1,k}_n + \frac{\tilde{K}^{j+1,k}_{n+1/2}}{\Delta z_n} + \frac{\tilde{K}^{j+1,k}_{n-1/2}}{\Delta z_{n-1}} \right) \tilde{\psi}^{j+1,k+1}_n \\
&\quad - \frac{\tilde{K}^{j+1,k}_{n+1/2}}{\Delta z_n} \tilde{\psi}^{j+1,k+1}_{n+1} = \frac{\overline{\Delta z_n}}{\Delta t^j} \tilde{C}^{j+1,k}_n \tilde{\psi}^{j+1,k}_n - \frac{\overline{\Delta z_n}}{\Delta t^j} \left(\tilde{\theta}^{j+1,k}_n - \theta^j_n \right) \\
&\quad + \left(\tilde{K}^{j+1,k}_{n+1/2} - \tilde{K}^{j+1,k}_{n-1/2} \right) - \overline{\Delta z_n} S^j_n, \quad n = 2, \ldots, N_z - 1, \qquad (4.4)
\end{aligned}
$$

together with two additional equations for $n = 1, N_z$, related to the discretized boundary conditions.

The iteration procedure explained above, in combination with the finite difference spatial approximation, leads to simple sets of tridiagonal linear systems for computing the numerical solution. This special property of our method contrasts with the typical banded structure of the systems which appear in the classical implicit methods (see [1, 3, 5, 8]), reducing drastically the computational cost of the resolution process and allowing a natural implementation in parallel devices with maximum speed-up.

5. Numerical Experiment

The numerical test described below corresponds to a simulation of a lixiviation model which takes place from a contaminant source to an unconfined aquifer with a pumping well. The geometry of the system is shown in the plant and section views of Fig. 1, defining a flow domain $\Omega = [0, 260] \times [-50, 50] \times [0, 38]$.

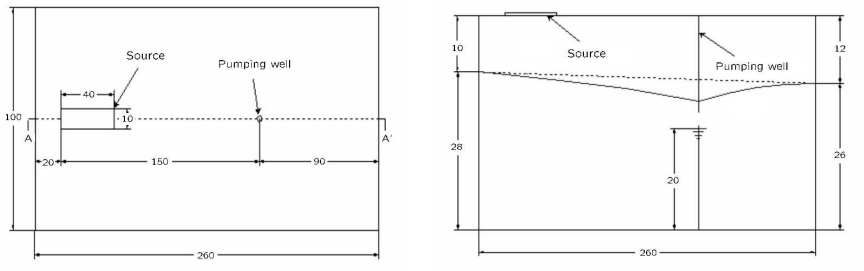

a) b)

Figure 1. Plant and section views of the flow domain (dimensions are expressed in meters).

As initial condition, we have considered a phreatic layer which varies linearly from 28 m on the left margin of the aquifer to 26 m on the right one (i.e., $\psi(\mathbf{x}, 0) = 28 - x/130 - z$). Moreover, $\psi + z = 28$ and $\psi + z = 26$ are assumed as boundary restrictions for $x = 0$ and $x = 260$, respectively ($y \in [-50, 50]$). The lixiviation process starts at a time in which the water table descends to

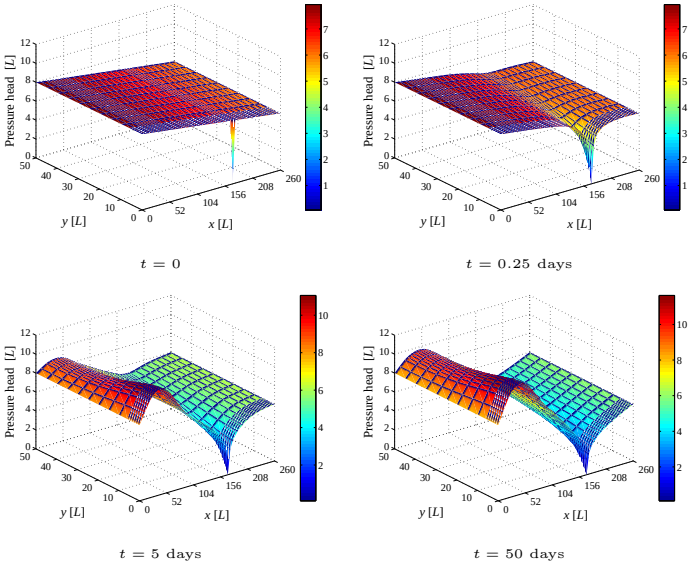

Figure 2. Evolution of the pressure head ψ at the plane $z = 20$.

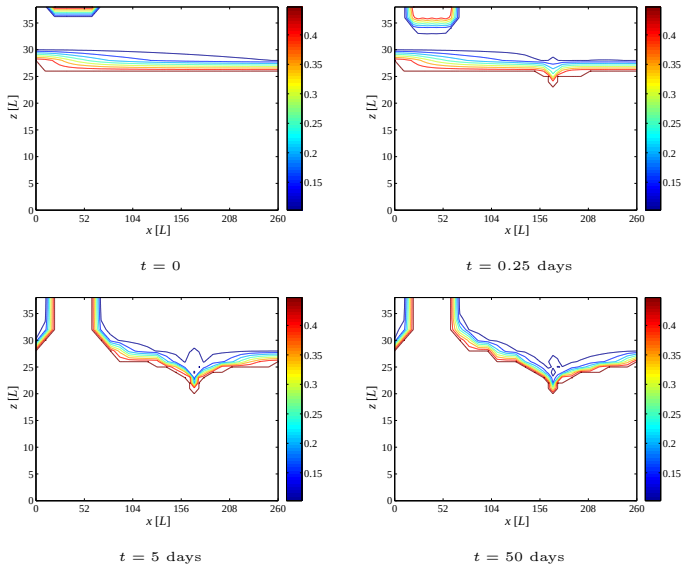

Figure 3. Evolution of the moisture content θ at the plane $y = 0$.

20 m at the segment that contains the pumping well ($x = 170$, $y = 0$). Hence, this segment is characterized by the boundary condition $\psi + z = 20$ along the vertical below the phreatic layer ($z \leq 20$), assuming the development of a filtration line above its position ($z > 20$) (i.e., we impose $\psi = 0$ under satu-

ration conditions, considering zero vertical flux for the unsaturated nodes). Finally, a $\psi = 0$ condition is assumed at the contaminant source, assigning impermeability restrictions on the other boundary surfaces.

Numerical results are described in Figs. 2 and 3. Note that, due to the symmetry of the system with respect to the plane $y = 0$, we have considered just one half of the flow domain in the simulation. At first, Fig. 2 represents the evolution of ψ at the plane $z = 20$. From a given initial distribution $\psi(\mathbf{x}, 0) = 8 - x/130$, the pressure head shows a progressive growth at the source position and the generation of a depression cone around the pumping well. This process reveals the existence of a time-dependent flux between these devices until the stationary state is reached. On the other hand, Fig. 3 describes the evolution of θ at the plane $y = 0$. In this case, the configuration of the moisture content isolines shows a tracking front movement towards the phreatic layer position. According to the numerical experiments, the steady state is reached approximately 40 days after the beginning of the simulation.

References

[1] A. Arrarás. Hydrofem: A three-dimensional model for simulating water flow in variably saturated porous media. In: J. Álvarez-Benedí and P. Marinero(Eds.), *Proc. of the 6-th Intern. Conference on the Unsaturated Zone of Soil ZNS-03, Valladolid, Spain, 2003*. Valladolid, 271 – 278, 2003.

[2] B. Bujanda and J.C. Jorge. Stability results for linearly implicit fractional step discretizations of non-linear time dependent parabolic problems. *App. Num. Math.* (article in press)

[3] M.A. Celia, E.T. Bouloutas and R.L. Zarba. A general mass-conservative numerical solution for the unsaturated flow equation. *Water Resour. Res.*, **26**(7), 1483 – 1496, 1990.

[4] R.A. Feddes, P. Kabat, P.J.T. Van Bakel, J.J.B. Bronswijk and J. Halbertsma. Modelling soil water dynamics in the unsaturated zone: state of the art. *J. Hydrol.*, **100**(1), 69 – 111, 1988.

[5] R.A. Feddes, S.P. Neuman and E. Bresler. Finite element analysis of two-dimensional flow in soils considering water uptake by roots: I. Theory. *Soil Sci. Soc. Am. Proc.*, **39**(2), 224 – 230, 1975.

[6] F. Lisbona, G. Aguilar, C. Clavero and J.L. Gracia. *Modelling and Simulation of Capillary Barriers*. ENRESA Technical Publication 08, 1998. (In Spanish)

[7] C. Paniconi, A.A. Aldama and E.F. Wood. Numerical evaluation of iterative and noniterative methods for the solution of the nonlinear Richards' equation. *Water Resour. Res.*, **27**(6), 1147 – 1163, 1991.

[8] G.F. Pinder and W.G. Gray. *Finite Element Simulation in Surface and Subsurface Hydrology*. Academic Press, Inc., 1977.